Analysis & Control Design *vs* Saturations
Phase Plane & Describing Function Methods

J-M. Biannic

http://www.onera.fr/staff/jean-marc-biannic
http://jm.biannic.free.fr

MASTER OF AEROSPACE ENGINEERING

ONERA THE FRENCH AEROSPACE LAB

isae Institut Supérieur de l'Aéronautique et de l'Espace SUPAERO

General context

Linear control theory has now reached a high level of maturity despite a few remaining obstacles (high dimension, multiple objectives, ...). Moreover, direct extensions of linear strategies (gain scheduling, self scheduling, LPV control, dynamic inversion, adaptive control) enable to solve a large class of **aerospace control problems**.

There remain however a few (but unfortunately ubiquitous) nonlinearities which cannot be linearized:

- magnitude & rate saturations
- deadzone functions
- relays (possibly including hysteresis)

Considered systems in this course

In this introduction to saturated plants, one focuses on systems with the following structure:

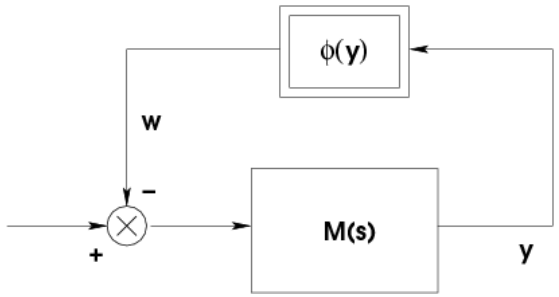

where $\phi(.)$ is a **static**, piecewise affine nonlinearity. Typically, it can be a saturation, a deadzone, a relay...

Remark #1 Dynamic nonlinearities such as rate limiters can be transformed into static ones.

Remark #2 Any static nonlinearity cadn be approximated by a piecewise affine function.

General Content

The course is organized in three parts. The first two ones are dedicated to the stability analysis and limit cycles detection in the nonlinear systems described above. The last part is dedicated to a short presentation of the anti-windup structure.

- stability analysis with the phase plane technique
- limit-cycle detection with the describing function method
- anti-windup design

Content

Phase plane method: general principle

The phase plane method "simply" consists in plotting a set of trajectories (the phase portrait) of the nonlinear system in the state space (the phase plane) in order to characterize its **stability domain**[1].

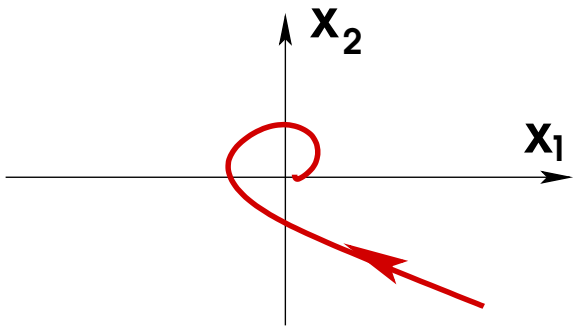

Phase portrait of a linear system

$$\dot{x} = A\,x$$

Stability domain : $\mathbb{R}^2$

In practice, this method is then restricted to second-order plants. But interestingly, it permits to obtain an exact characterization of the stability domain in the presence of any piecewise affine nonlinearity.

[1] The stability of a nonlinear system is often guaranteed locally on a restricted region (or possibly several) of the state space

Construction of a phase portrait: 4 steps

After setting the system in the appropriate format the construction of a phase portrait requires 4 steps:

- Step 1 : Determine the critical points by computing:

$$\dot{x} = Ax - B\phi(y) = 0$$

- Step 2 : Identify the regions in the phase plane induced by the segments of the piecewise affine nonlinearity $\phi(.)$,
- Step 3 : In each region compute and plot the trajectories about each critical point,
- Step 4 : Connect the trajectories and identify the stability domain.

Equations

The linear system $M(s)$ in negative feedback loop with $\phi(.)$ is described by the set of equations:

$$\begin{cases} \dot{x} = \begin{bmatrix} 0 & 1 \\ a_1 & a_2 \end{bmatrix} x + \begin{bmatrix} 0 \\ 1 \end{bmatrix} u \\ y = \begin{bmatrix} c_1 & c_2 \end{bmatrix} x \\ u = -\phi(y) \end{cases}$$

The nonlinearity is piecewise affine:

$$y \in I_i \;\Rightarrow\; \phi(y) = \alpha_i y + \beta_i$$

If y belongs to the interval I_i, the system verifies:

$$\dot{x} = \underbrace{\begin{bmatrix} 0 & 1 \\ a_1 - \alpha_i c_1 & a_2 - \alpha_i c_2 \end{bmatrix}}_{A_i} x - \underbrace{\begin{bmatrix} 0 \\ \beta_i \end{bmatrix}}_{B_i}$$

Critical points

The critical points are obtained with the following equation:

$$\dot{x} = A_i x - B_i = 0$$

Since the system is not described by a unique differential equation but a family of equations, one obtains a discrete set of critical points (when A_i is invertible):

$$x_{S_i} = A_i^{-1} B_i = \begin{bmatrix} \frac{\beta_i}{a_1 - \alpha_i c_1} \\ 0 \end{bmatrix}$$

Phase plane regions

The region $\mathcal{R}_i$ in the phase plane is defined by the set of points whose coordinates satisfy $Cx \in I_i$. As illustrated below, the borders are parallel lines.

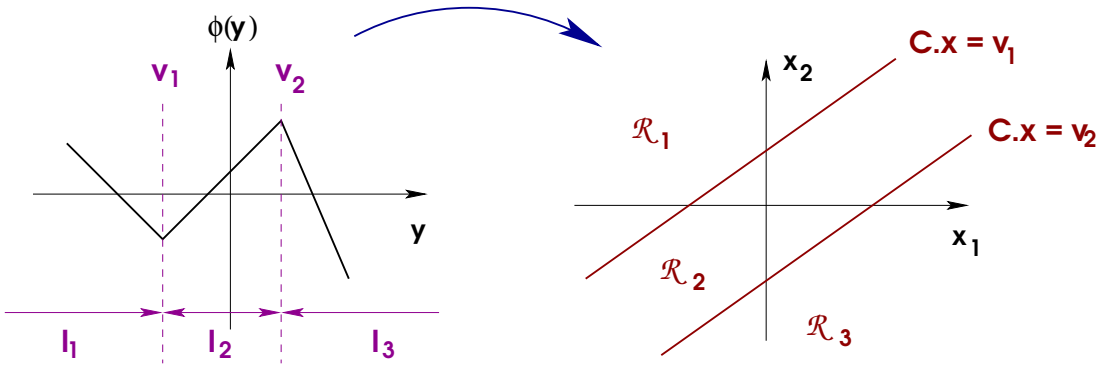

Remark: *In most cases, the critical point S_i belongs to the region $\mathcal{R}_i$. In some cases, this is not satisfied. In that case we have a* **virtual** *critical point.*

Trajectories

Near a critical point S_i, after a translation, the trajectories verify a **linear** differential equation:

$$\dot{\xi} = A_i \xi \ , \quad x = \xi + x_{S_i}$$

Despite this simple formulation, it remains somewhat tricky to characterize the trajectories (to plot x_2 as a function of x_1). The most common exercise consists indeed to plot time-domain responses...

Despite the reduced dimension of A_i (2×2), 6 cases (in non degenerated cases) must be considered according to the values of λ_1 and λ_2 in the complex plane.

Trajectories : The six (non-degenerated) cases

Distinct real eigenvalues

$\lambda_1 > 0,\ \lambda_2 > 0$	**Unstable node** parabolic divergent trajectories
$\lambda_1 < 0,\ \lambda_2 < 0$	**Stable node** parabolic convergent trajectories
$\lambda_1 \lambda_2 < 0$	**Saddle point** hyperbolic trajectories

Complex eigenvalues

$\mathcal{R}e(\lambda_i) < 0$	**Stable spiral** convergent spiral trajectories
$\mathcal{R}e(\lambda_i) > 0$	**Unstable spiral** divergent spiral trajectories
$\mathcal{R}e(\lambda_i) = 0$	**Center** elliptic trajectories

Trajectories : The six non-degenerated cases

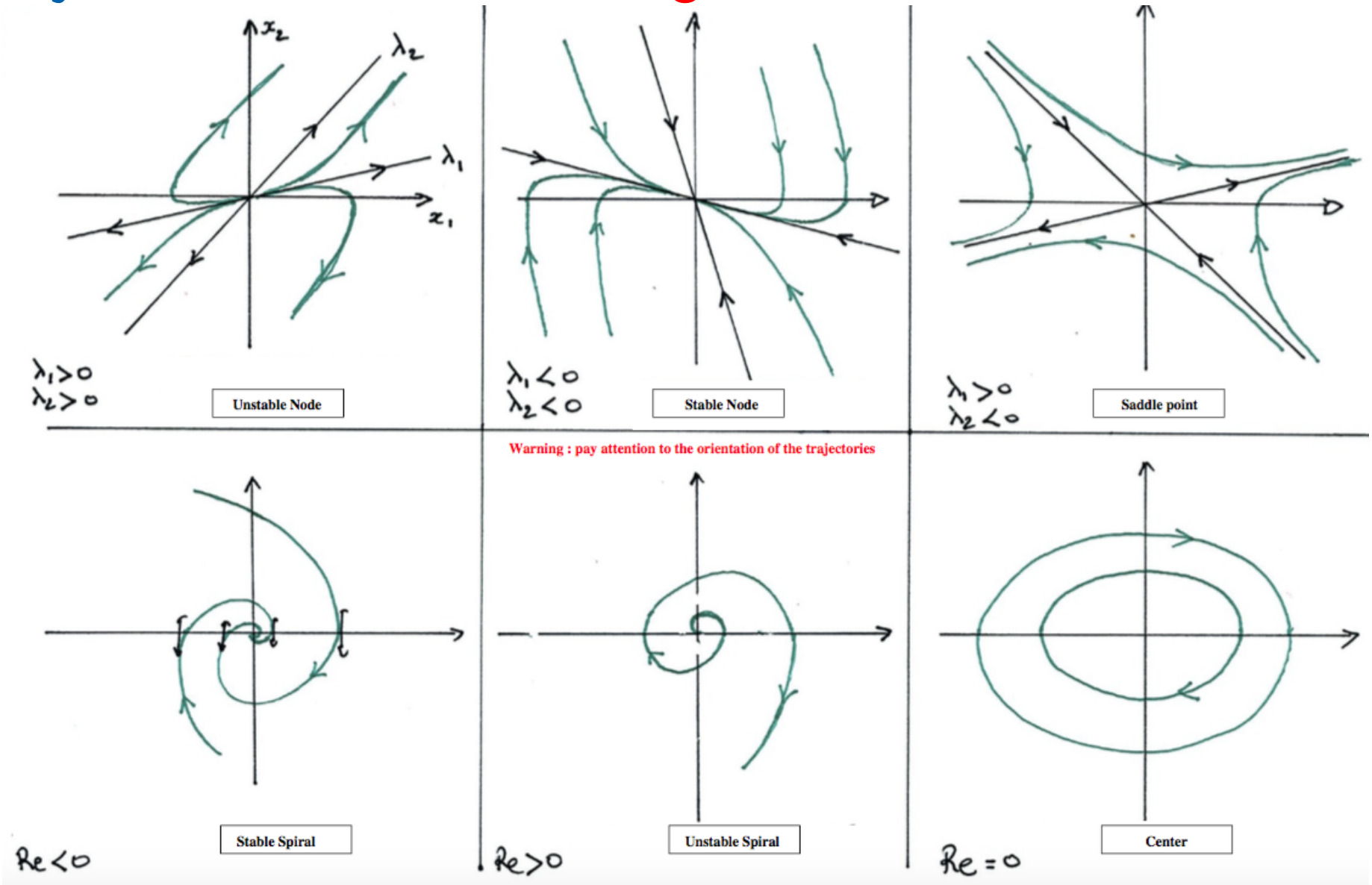

Phase portrait : An example

One considers the following system:

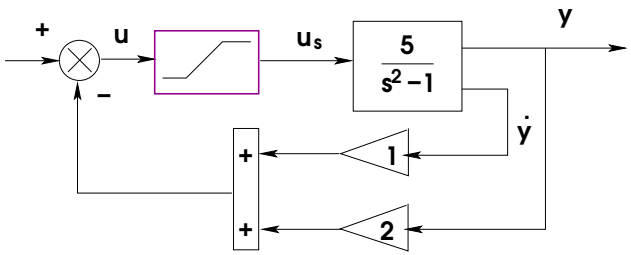

where the saturation is assumed unitary and symmetric. Setting $x_1 = y$ and $x_2 = \dot{y}$, one obtains:

$$\begin{cases} \dot{x}_1 = x_2 \\ \dot{x}_2 = x_1 - 5\mathbf{sat}(2x_1 + x_2) \end{cases}$$

which is in the appropriate format.

Conclusions on the phase plane method

- The phase portrait of the above system clearly illustrates the impact of saturations on the size of the stability domain. This impact is significant since the plant is open-loop unstable.
- The phase-plane technique is quite interesting to get a better understanding of the nonlinear effects and the best way to counteract them,
- Unfortunately, it is only applicable to second-order plants and it is quite difficult to extend it to higher-order models or to use it to automatize a nonlinear design process

Content

Motivating example

Consider again the above unstable system in feedback loop with a stabilizing proportional-derivative controller.

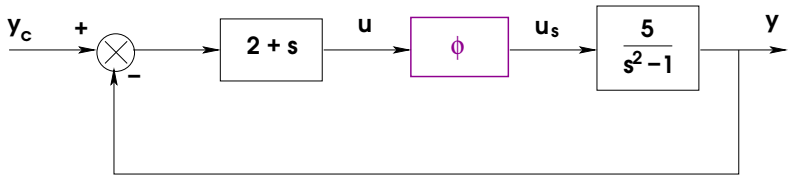

We noticed with the phase-plane technique that if Φ represents a magnitude saturation, then the size of the stability domain is reduced. We would like now to characterize the effects of a **rate saturation**. The problem is that the characterization of this **dynamic** nonlinearity requires an additional state.

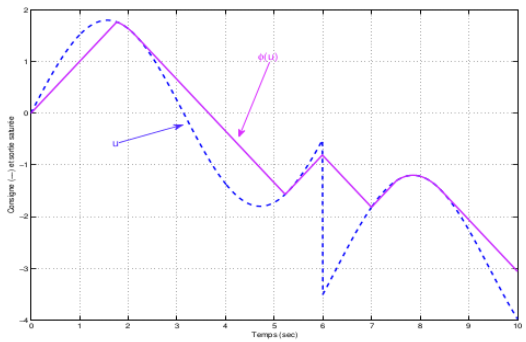

$$\Phi(u) < u \Rightarrow \dot{\Phi} = L$$
$$\Phi(u) > u \Rightarrow \dot{\Phi} = L$$
$$\Phi(u) = u \Rightarrow \begin{cases} \dot{\Phi} = \dot{u} \text{ si } |\dot{u}| \leq L \\ \dot{\Phi} = sign(\dot{u}).L \text{ si } |\dot{u}| > L \end{cases}$$

Motivating example

The above characterization is not easily compatible with the phase plane approach for which static nonlinearities are highly preferable. But we notice that the rate saturation can be approximated as follows (with small τ):

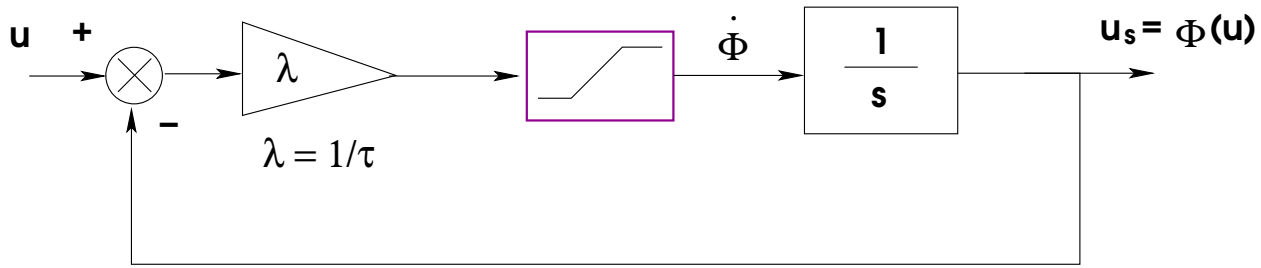

We thus obtain:

$$\dot{\Phi} = \text{sat}\left(\lambda(u - \Phi)\right)$$

where the rate saturation is replaced by a standard magnitude saturation encapsulated in a first-order closed-loop system (then involving as previously an additional state).

Motivating example

The nonlinear system is then now described by the following equations:

$$\begin{cases} \dot{x}_1 = x_2 \\ \dot{x}_2 = x_1 + 5\Phi \\ \dot{\Phi} = \mathsf{sat}\left(\lambda(u - \Phi)\right) = -\mathsf{sat}\left(\lambda(2x_1 + x_2 + \Phi)\right) \end{cases}$$

The analysis of such a system with the phase plane technique becomes tricky since a 3D space must now be considered, even if the number of regions (3) to be studied has remained unchanged:

$$\begin{aligned} \mathcal{R}_1 &: |2x_1 + x_2 + \Phi| \leq \tau \\ \mathcal{R}_2 &: 2x_1 + x_2 + \Phi > \tau \\ \mathcal{R}_3 &: 2x_1 + x_2 + \Phi < -\tau \end{aligned}$$

Motivating example

For each region $\mathcal{R}_i$, the system is described by:

$$\dot{x} = A_i x + b_i$$

with:

$$A_1 = \begin{pmatrix} 0 & 1 & 0 \\ 1 & 0 & 5 \\ -2\lambda & -\lambda & -\lambda \end{pmatrix} \ , \ b_1 = \begin{pmatrix} 0 \\ 0 \\ 0 \end{pmatrix}$$

$$A_2 = A_3 = \begin{pmatrix} 0 & 1 & 0 \\ 1 & 0 & 5 \\ 0 & 0 & 0 \end{pmatrix} \ , \ b_2 = -b_3 = \begin{pmatrix} 0 \\ 0 \\ -1 \end{pmatrix}$$

The phase portrait is difficult to obtain for the following reasons:

- dimension > 2,
- no singular point in $\mathcal{R}_2$ nor in $\mathcal{R}_3$ where the system behavior is characterized by the characteristic polynomial $\psi(s) = s(s^2 - 1)$ (3 poles are obtained : $\lambda_1 = 0$, $\lambda_2 = 1$, $\lambda_3 = -1$).

Motivating example

A 3D trajectory for a given initial condition is visualized below:

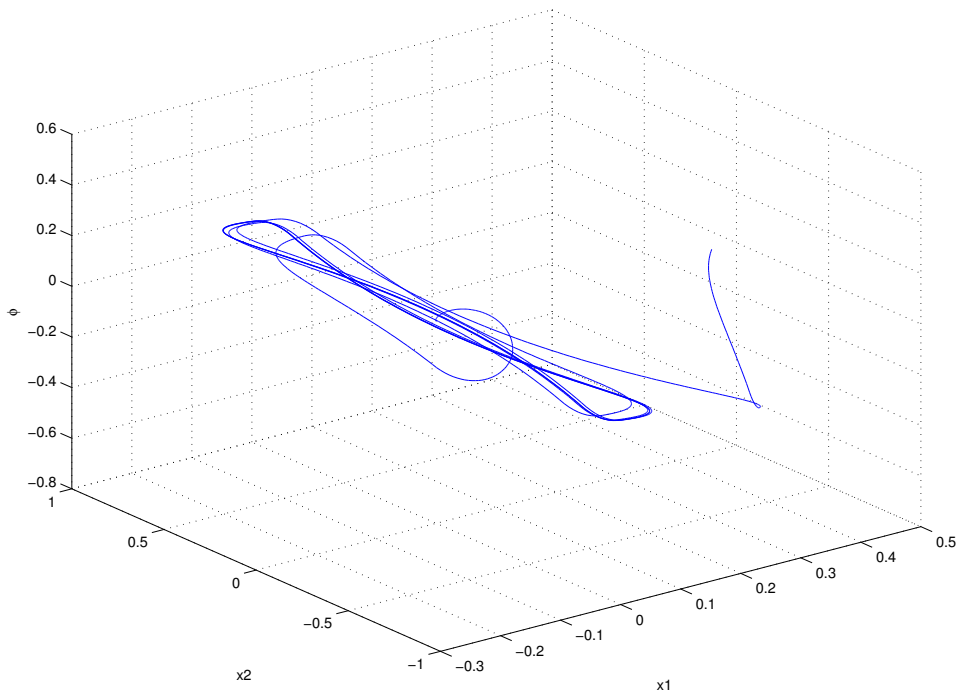

...and seems difficult to exploit at first glance...

Motivating example

But let us now observe the 2D-projections of the above trajectory:

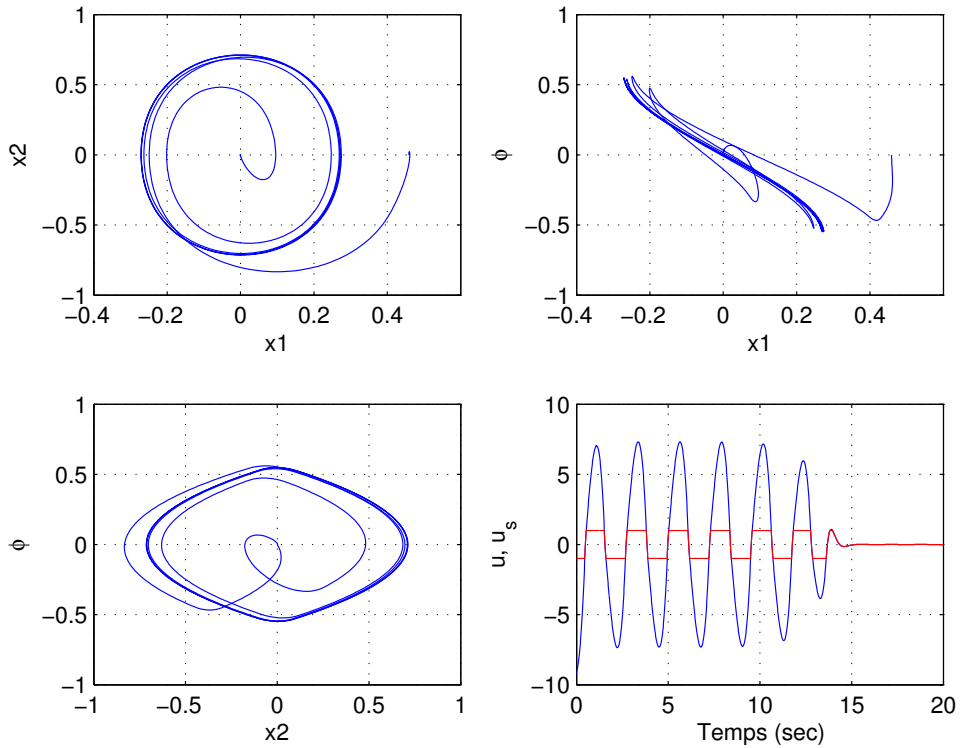

A specifically nonlinear oscillatory behavior known as a **limit-cycle**, is clearly highlighted.

Motivating example

A MATLAB démo enables to confirm the existence of this **closed trajectory** and to check that its characteristics (magnitude and perdiod) do not depend on the initial conditions. Such a property is specific to limit-cycles unlike oscillations in marginally stable linear systems whose magnitude depend on the initial condition.

We note here that according to the chosen initial conditions, in a neighborhood of the limit-cycle, the system trajectories either converge to the origin or diverge after a transient response near to the limit-cycle trajectory. Then we have an **unstable limit-cycle**.

Remark: *Stable (or attractive) limit-cycles may also exist. In such a case, the system trajectories converge to the limit-cycle. Their stability can be local or global.*

Motivating example

On our example the detection of an unstable limit cycle has a high practical interest since the latter locally separates the state space into two regions. For some initial condition located in one of these two regions, a stable trajectory will be obtained while trajectories starting from the other region will be unstable.

Then the magnitude of the limit cycle (distance to the origin) will indirectly characterize the size of the stability domain about the origin. This characterization is exact for 2D systems.

The detection of a limit cycle, its property (stable or unstable) and characteristics (magnitude and pulsation) has a high interest for stability analysis of nonlinear systems. In our example, such a limit cycle was identified by intensive numerical simulations. In the case of high order systems, this approach becomes tedious...

Motivating example

Let us then develop an input/output methodology whose complexity will not increase with the order of the system. To this purpose, let us open the loop at the input and output of the saturation nonlinearity.

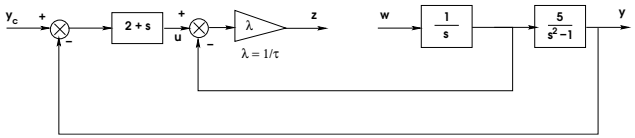

One obtains:

$$z = -\lambda \frac{s^2 + 5s + 9}{s(s^2 - 1)} w = -G(s)w$$

and the simplified diagram may be considered for stability analysis:

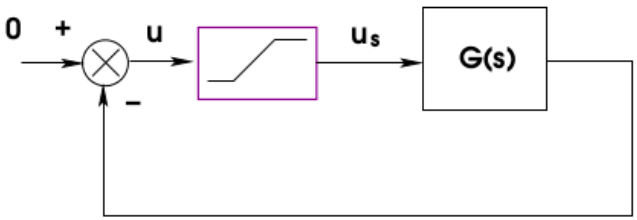

$$G(s) = \lambda \frac{s^2+5s+9}{s(s^2-1)}$$

Motivating example

Replacing the saturation by a **real gain** $k(u) \in]0, 1]$:

$$u_s = sat(u) = k(u).u = \min(1, 1/|u|).u$$

it seems that the analysis **could** be performed with the help of a root locus of $F(s) = \frac{s^2+5s+9}{s(s^2-1)}$ which is drawn below:

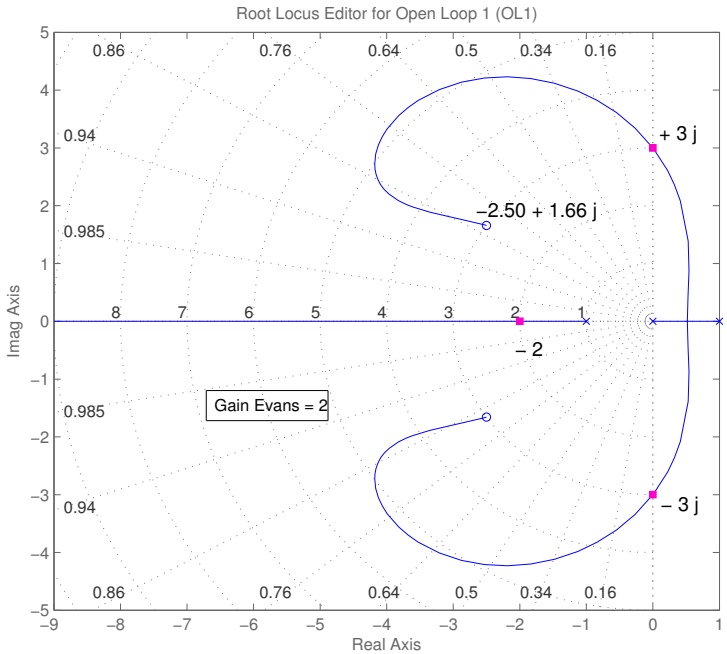

Motivating example

The root locus reveals a singularity for $\omega_c = 3$ and $gain = 2$, *i.e* $\lambda k = 2$. The limit of stability is then reached for:

$$k(u) = \frac{2}{\lambda}$$

If the gain λk increases, then $k(u)$ increases and the system becomes stable. The magnitude of $|u|$ will also decrease as well as the saturation activity. Conversely, if the gain λk decreases then the system becomes unstable, $|u|$ increases as well as the saturation activity. In both cases, the system will not remain close to the limit-cycle which is clearly unstable.
In an **LTI** framework, the magnitude of the limit-cycle **would** be obtained as follows:

$$k(u) = \frac{2}{\lambda} = \frac{1}{|u|} \Rightarrow |u| = \frac{\lambda}{2}$$

Motivating example

Let us now compare the above "theoretical" results with the "experimental" reality for $\lambda = 10$. The theoretical values are: $u_{0_{th}} = 5$ and $\omega_{c_{th}} = 3$

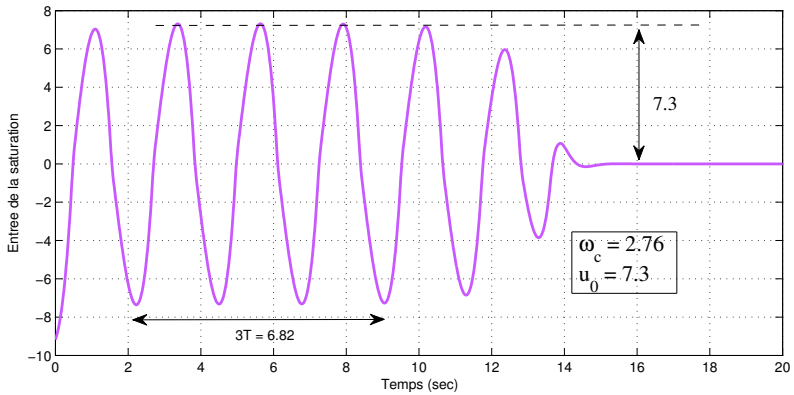

One observes 10% on the pulsation and 30% error on the magnitude which is quite significant. The problem comes from the wrong interpretation of the gain $k(u)$ as a static gain, while in the real system, this is a **time-varying** gain: $k(u) = k(u(t))$.

Objectives & principle

The objective of the first harmonic method is to detect and characterize oscillations (**limit-cycles**) in nonlinear systems. The general principle of the approach is rather close to what has been presented in the introduction with fundamental differences though, through the following assumptions and notions:

- first harmonic approximation,
- describing funcion

which will be detailed next.

General principle

The detection of **single-harmonic** permanent oscillations in nonlinear systems from our studied class with pulsation ω and magnitude u_0 boils down to checking the existence of a signal $u_0 sin(\omega t)$ at the input of the nonlinearity which coincides to the opposite of the signal at the output of $G(s)$.

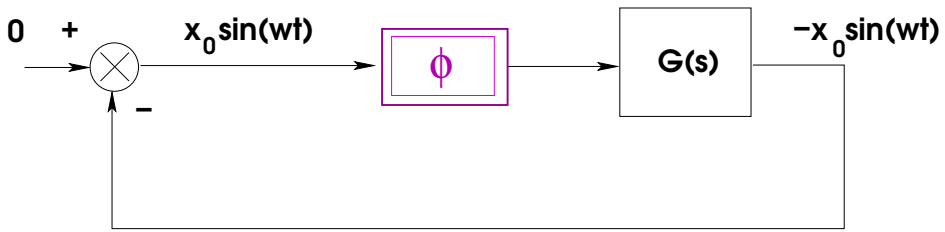

Assuming that the nonlinearity can be represented by an equivalent (possibly complex-valued) gain $N = \rho e^{j\varphi}$ (the describing function) such that $u_s = \rho u_0 sin(\omega_t + \varphi)$, the condition for the existence of a limit-cycle is simply given by:

$$GN = -1$$

Describing function

Transmission of a sinusoidal input in a nonlinear system

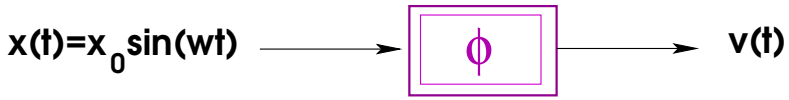

Fourier's Serie Development:

$$\begin{aligned} v(t) &= v_0 + \sum_{k\geq 1} v_k \sin(k\omega t + \varphi_k) \\ &= v_0 + \sum_{k\geq 1} a_k \sin(k\omega t) + \sum_{k\geq 1} b_k \cos(k\omega t) \end{aligned}$$

with:

$$a_k = \frac{2}{T}\int_0^T v(t)\sin(k\omega t)\,dt$$

$$b_k = \frac{2}{T}\int_0^T v(t)\cos(k\omega t)\,dt$$

$$v_0 = \frac{1}{T}\int_0^T v(t)\,dt$$

Describing function

First Harmonic Approximation

$$v(t) \approx v_0 + a_1 \sin(\omega t) + b_1 \cos(\omega t)$$

Using complex notation:

$$v \approx v_0 + Nx$$

with:

$$N = \frac{a_1 + jb_1}{x_0} = \frac{2j}{Tx_0} \int_0^T v(t) e^{-j\omega t}\, dt$$

A priori, the **Sinusoidal Input Describing Function** (SIDF) Φ depends on both the magnitude x_0 and the pulsation ω.

Describing function

In the case of a **static** nonlinearity, the signal reads $v(t) = \Phi(x_0 \sin(\omega t))$. The output of the nonlinearity at each time instant depends only on the magnitude of the input at the same time. In the general expression of the describing function the following change of variable $\omega t = u$, can be performed such that :

$$v(t) = \Phi(x_0 \sin u)$$

Finally :

$$N = \frac{j}{\pi x_0} \int_0^{2\pi} \Phi(x_0 \sin u) e^{-ju}\, du = N(x_0)$$

which shows that the describing function only depends on x_0.

Describing function : practical approach

We first compute a_1 and b_1 to derive $N = (a_1 + jb_1)/x_0$. In the case of **static nonlinearities** :

$$a_1 = \frac{1}{\pi} \int_0^{2\pi} \Phi(x_0 \sin u) \sin u \, du$$

$$b_1 = \frac{1}{\pi} \int_0^{2\pi} \Phi(x_0 \sin u) \cos u \, du$$

Remark : for odd nonlinearities $(\Phi(-x) = -\Phi(x))$ such as symetrical relays or saturations for example we easily verify that $b_1 = 0$ and the equivalent gain is then **real**.

Describing function of a relay

We consider the symetrical relay function with magnitude M

$$\Phi(x) = M.\text{sign}(x)$$

- $a_1 = \frac{1}{\pi}\int_0^{\pi} M \sin u \, du - \frac{1}{\pi}\int_{\pi}^{2\pi} -M \sin u \, du$

$$\Rightarrow a_1 = \frac{4}{\pi}\int_0^{\frac{\pi}{2}} M \sin u \, du = \frac{4M}{\pi}$$

- $b_1 = 0$

Equivalent gain of a relay

$$N_{relais}(x_0) = \frac{4M}{\pi x_0}$$

Describing function of a saturation

We consider the symetrical relay function with magnitude L

$$\Phi(x) = \begin{cases} x & \text{si } |x| \leq L \\ L.\text{sign}(x) & \text{si } |x| > L \end{cases}$$

We assume $x_0 > L$ and define θ such that $x_0 \sin(\theta) = L$. Thus :

$$u \in [0\,,\ \theta] \Rightarrow \Phi(x_0 \sin u) = x_0 \sin u\ , \quad u \in [\theta\,,\ \pi/2] \Rightarrow \Phi(x_0 \sin u) = L$$

- $$a_1 = \frac{4}{\pi}\int_0^{\theta} x_0 \sin^2 u\, du + \frac{4}{\pi}\int_{\theta}^{\frac{\pi}{2}} L \sin u\, du$$

$$\Rightarrow a_1 = \frac{2x_0}{\pi}(\theta + \sin\theta\cos\theta)$$

Equivalent gain of a saturation

$$N_{sat}(x_0) = \frac{2}{\pi}\left(\arcsin\frac{L}{x_0} + \frac{L}{x_0}\sqrt{1 - \frac{L^2}{{x_0}^2}}\right) \underset{x_0 \gg L}{\approx} \frac{4L}{\pi x_0}$$

Describing function of a relay with hysteresis

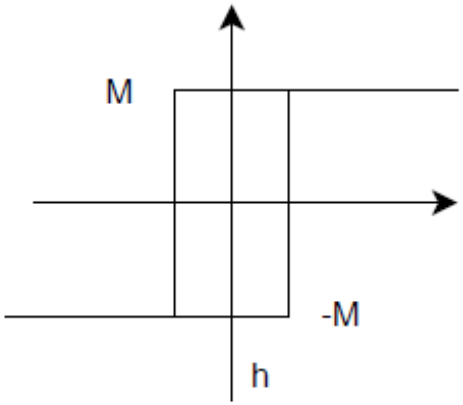

$$x_0 \sin\theta = h$$

$$u \in [0\,,\ \theta] \Rightarrow \Phi(x_0 \sin u) = -M$$

$$u \in [\theta\,,\ \pi] \Rightarrow \Phi(x_0 \sin u) = +M$$

- $a_1 = \dfrac{2}{\pi}\displaystyle\int_0^{\theta} -M \sin u\, du + \frac{2}{\pi}\int_{\theta}^{\pi} M \sin u\, du = \frac{4M}{\pi}\cos\theta$
- $b_1 = \dfrac{2}{\pi}\displaystyle\int_0^{\theta} -M \cos u\, du + \frac{2}{\pi}\int_{\theta}^{\pi} M \cos u\, du = -\frac{4M}{\pi}\sin\theta$

$$\Rightarrow N_{rh}(x_0) = \frac{a_1 + jb_1}{x_0} = \frac{4M}{\pi x_0}(\cos\theta - j\sin\theta) = \frac{4M}{\pi x_0}e^{-j\theta}$$

Describing function of a relay with hysteresis

Equivalent gain of a relay with hysteresis

$$N_{rh}(x_0) = \frac{4M}{\pi x_0} e^{-j \arcsin(h/x_0)}$$

Remark :

$$-\frac{1}{N_{rh}(x_0)} = -\frac{\pi}{4M}\sqrt{x_0^2 - h^2} - j\frac{\pi h}{4M}$$

The critical locus of the relay with hysteresis is visualized in red on the figure below.

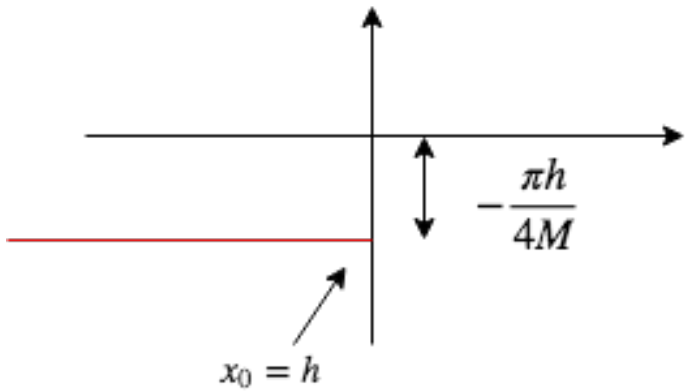

Limit-cycle detection

The limit cycle detection with static nonlinearities is easy since the critical locus is only parameterized in x_0 while the Nyquist locus of the linear system depends only on ω.
Then we have :

$$G(j\omega_c) = -\frac{1}{N(x_0)} \tag{1}$$

from which ω_c is readily obtained and next, the gain :

$$N(x_0) = -\frac{1}{G(j\omega_c)} \tag{2}$$

From the last relation, we easily deduce the magnitude x_0 of the limit cycle via the reciprocal function $N^{-1}(.)$. So we have :

$$x_0 = N^{-1}\left(-\frac{1}{G(j\omega_c)}\right) \tag{3}$$

Back to the example

$$G(s) = 10\,\frac{s^2+5s+9}{s(s^2-1)} \;\Rightarrow\; G(j\omega) = -10\,\frac{9-\omega^2+5j\omega}{j\omega(1+\omega^2)}$$

The Nyquist locus of $G(s)$ intersects of the critical locus of saturation nonlinearity on the x-axis $]-\infty,\,-1]$ for a pulsation ω_c such that $\mathcal{I}m(G(j\omega_c)) = 0$. For $\omega = \omega_c = 3$, we obtain :

$$G(j\omega_c) = -10\frac{5}{1+9} = -5 = -\frac{1}{N(x_0)}$$

For a saturation with amplitude L :

$$N(x_0) \approx \frac{4L}{\pi x_0} \Rightarrow x_0 \approx \frac{20}{\pi} \approx 6.4$$

This value is rather close to the exact one.

Summary of the approach

1. Extract the linear part $G(s)$ that is seen by the nonlinearity with a **negative feedback** (usual convention to compute margins),
2. Compute the equivalent gain of the nonlinearity and deduce the critical locus,
3. Compute the intersection (ω_c, x_c) in the complex plane between the critical locus of the nonlinearity (that depends on x_0 in the static case) and the Nyquit plot of $G(s)$ (that depends on ω)
4. Characterize the property of each intersection (stable/unstable),
5. Verify the quality of the approaximation (attenuation of higher harmonics) :

$$\forall k \geq 2, \tau_k = \frac{|G(kj\omega_c)|}{|G(j\omega_c)|} < 0.1 \ ?$$

General scheme

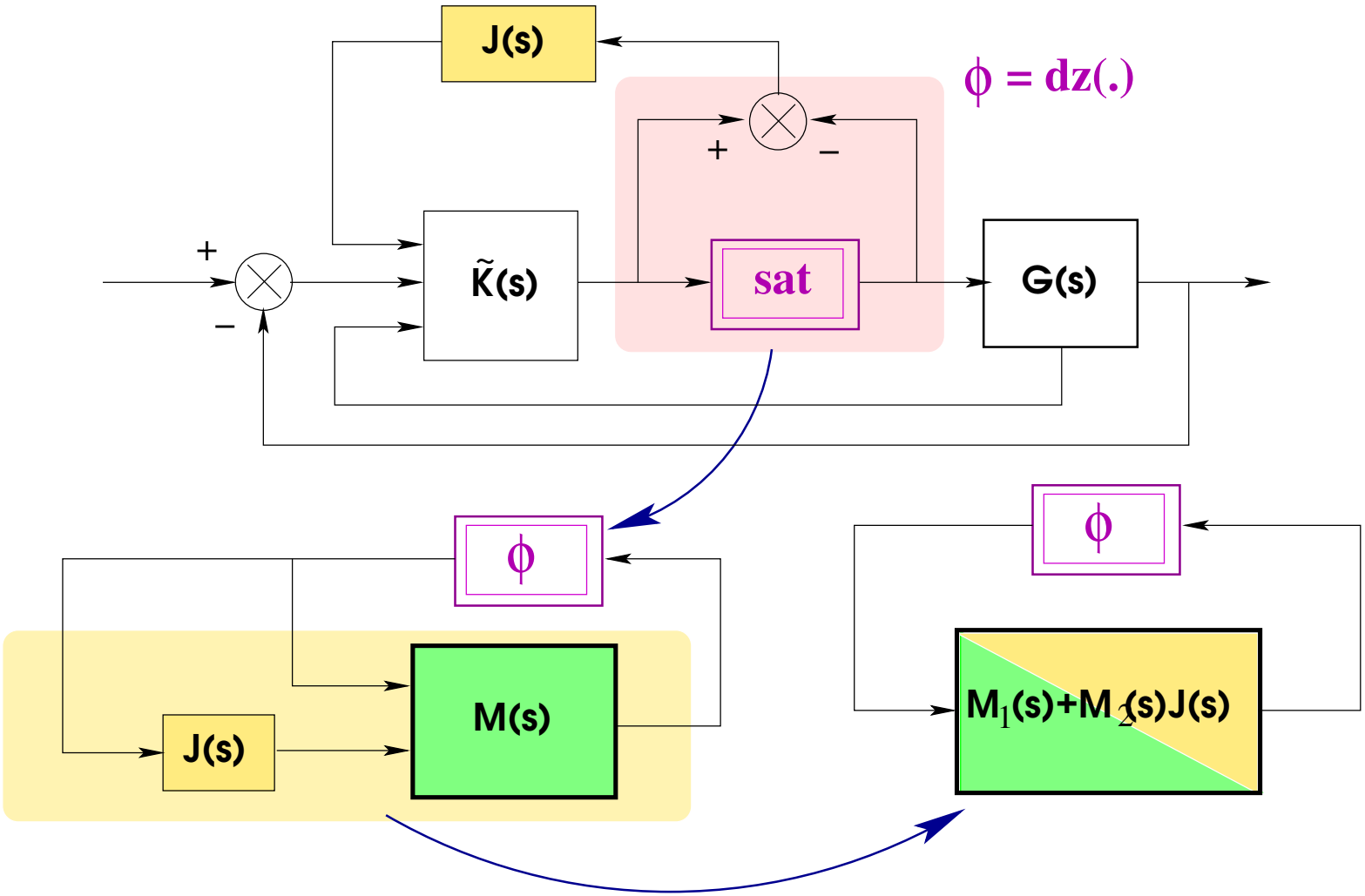

Describing function analysis

From the above scheme (**linear anti-windup architecture**), the analysis of an anti-windup compensator (after integration in an augmented plant and assuming that a given saturation is dominant so that the others can be neglected) can be realized by the first-harmonic approximation method.

Once the anti-windup compensator $J(s)$ is fixed, the nonlinear system to be analyzed assumes a standard form $\mathcal{M}(s) - \phi$ with:

$$\mathcal{M}(s) = M_1(s) + M_2(s)J(s)$$

The detection of limit-cycles is then achieved from the analysis of the Nyquist plot of $\mathcal{M}(s)$.

A design strategy

Next, an anti-windup design strategy can be derived by appropriately modeling the Nyquist plot of $M_1(s)+M_2(s)J(s)$ in a neighborhood of the critical locus of the nonlinearity.

The main idea consists of managing the intersections between the Nyquist plot and the critical locus in order to modify the characteristics of the limit cycles (magnitude and pulsation).

In the case of an unstable limit-cycle, the objective is to increase its magnitude (or ideally to avoid any intersection) so as to increase the size of the stability domain. In the case of a stable limit-cycle (satellite attitude control for example), the central objective will be to manage the pulsation (to avoid interactions with flexible and sloshing modes for example) and then to minimize the magnitude.

Augmented flight control laws

The general method that we have just described will be applied to tune a longitudinal control system for a combat aircraft. The control design of a PID controller is initially performed in a linear framework without taking saturations into account. Next, the saturations effects are analysed and a unstable limit cycle is revealed with the first harmonic method (confirmed by simulations).

A static anti-windup device is then implemented to "reduce" the integral effect when saturations are detected. The gain of this anti-windup is tuned so as to modify the magnitude of the limit cycle. For a specific value of this gain, the magnitude reaches a maximum and the stability domain of the nonlinear closed loop system is (undirectly) enlarged. Numerical (simulation-based) experiements confirm this fact but also show that the gain can be further increased to further enlarge the domain. Unfortunately this last observation is not directly explained by the limit-cycle approach which only captures specific nonlinear phenomena.